



*Citation for published version:*

Barbosa, Al, Sampaio Barreto, A & Reis, N 2019, 'Transparent, Hydrophobic Fluorinated Ethylene Propylene Offers Rapid, Robust, and Irreversible Passive Adsorption of Diagnostic Antibodies for Sensitive Optical Biosensing', *ACS Applied Biomaterials*, vol. 2, no. 7, pp. 2780-2790. <https://doi.org/10.1021/acsabm.9b00214>

*DOI:*

[10.1021/acsabm.9b00214](https://doi.org/10.1021/acsabm.9b00214)

*Publication date:*

2019

*Document Version*

Peer reviewed version

[Link to publication](#)

This document is the Accepted Manuscript version of a Published Work that appeared in final form in *ACS Applied Bio Materials*, copyright © American Chemical Society after peer review and technical editing by the publisher. To access the final edited and published work see <https://pubs.acs.org/doi/10.1021/acsabm.9b00214>.

## University of Bath

### General rights

Copyright and moral rights for the publications made accessible in the public portal are retained by the authors and/or other copyright owners and it is a condition of accessing publications that users recognise and abide by the legal requirements associated with these rights.

### Take down policy

If you believe that this document breaches copyright please contact us providing details, and we will remove access to the work immediately and investigate your claim.

## Article

**Transparent, hydrophobic FEP Teflon offers rapid, robust and irreversible passive adsorption of diagnostic antibodies for sensitive optical biosensing**

Ana Isabel Barbosa, Augusto Sampaio Barreto, and Nuno Miguel Reis

*ACS Appl. Bio Mater.*, **Just Accepted Manuscript** • DOI: 10.1021/acsabm.9b00214 • Publication Date (Web): 22 May 2019Downloaded from <http://pubs.acs.org> on June 6, 2019**Just Accepted**

“Just Accepted” manuscripts have been peer-reviewed and accepted for publication. They are posted online prior to technical editing, formatting for publication and author proofing. The American Chemical Society provides “Just Accepted” as a service to the research community to expedite the dissemination of scientific material as soon as possible after acceptance. “Just Accepted” manuscripts appear in full in PDF format accompanied by an HTML abstract. “Just Accepted” manuscripts have been fully peer reviewed, but should not be considered the official version of record. They are citable by the Digital Object Identifier (DOI®). “Just Accepted” is an optional service offered to authors. Therefore, the “Just Accepted” Web site may not include all articles that will be published in the journal. After a manuscript is technically edited and formatted, it will be removed from the “Just Accepted” Web site and published as an ASAP article. Note that technical editing may introduce minor changes to the manuscript text and/or graphics which could affect content, and all legal disclaimers and ethical guidelines that apply to the journal pertain. ACS cannot be held responsible for errors or consequences arising from the use of information contained in these “Just Accepted” manuscripts.

1  
2  
3 **Transparent, hydrophobic FEP Teflon offers rapid, robust and**  
4 **irreversible passive adsorption of diagnostic antibodies for**  
5 **sensitive optical biosensing**  
6  
7  
8  
9

10  
11 Ana Isabel Barbosa,<sup>a</sup> Augusto Sampaio Barreto<sup>a</sup> and Nuno Miguel Reis<sup>a,b,\*</sup>  
12

13 <sup>a</sup> Department of Chemical Engineering, Loughborough University, Loughborough,  
14 Leicestershire, LE11 3TU, UK  
15  
16

17 <sup>b</sup> Department of Chemical Engineering, University of Bath, Claverton Down, Bath, BA2  
18 7AY, UK  
19  
20  
21  
22  
23  
24  
25  
26  
27  
28  
29  
30  
31  
32  
33  
34  
35  
36  
37  
38  
39  
40  
41  
42  
43  
44  
45  
46  
47  
48  
49  
50  
51  
52  
53  
54  
55  
56  
57  
58  
59  
60

**ABSTRACT**

Current literature data is scarce and somehow contradictory in respect to the suitability of ‘non-stick’ fluoropolymer surfaces for immobilisation of biomolecules. We have previously shown empirically that transparent FEP Teflon offers rapid and sensitive optical biosensing of clinically relevant biomarkers. This study shows for the first time a comprehensive experimental analysis of passive adsorption of diagnostics IgG antibodies on actual FEP Teflon microfluidic strips. Full equilibrium isotherms and kinetics for passive adsorption were studied and modelled using protein titration method using hundreds of multi-bore microfluidic strips for a range of temperatures, pH, ionic strengths and inner diameters, using both polyclonal and monoclonal antibody systems. Results were benchmarked against other plastic hydrophobic and glass hydrophilic surfaces. For the first time, it was shown quantitatively that the hydrophobicity of fluoropolymer surfaces encourages the passive adsorption of diagnostics antibodies for biosensing, being insensitive the temperature of incubation and ionic buffer strength. The mass of captured antigen increased with increasing antibody surface coverage up to ~400 ng/cm<sup>2</sup>, with an optimal adsorbed antibody activity for 45-69% of full monolayer coverage, matching results for other biosensing surfaces. The equilibrium was reached fast, within 5-10 min and surprisingly both the kinetics and equilibrium of antibody adsorption were dependent of the inner diameter of microcapillaries. This is a novel and relevant result that will generally impact on the design of miniaturised microfluidic biosensing devices. The antibody surface densities obtained with hydrophobic plastic surfaces were 2 to 4-fold lower than for a hydrophilic (glass) surface, however the former presented a multi-layered adsorption with a higher level of irreversibility as shown by the adsorption and desorption rates around one order of magnitude smaller than for glass, which is highly desirable for biosensing with surface-coated biomolecules.

*Keywords: antibody adsorption, Teflon® FEP, adsorption kinetics, microcapillary film, biosensing, microfluidics*

## 1. INTRODUCTION

Immobilisation of proteins by passive adsorption certainly remains the simplest and most scalable method for manufacturing plastic immunosensing surfaces, however several limitations of this protein immobilisation technique have been identified in literature, such as specificity to surface chemistry, limited surface area available for binding, surface geometry, pH, temperature and buffer ionic strength.<sup>1</sup> Consequently, manufacturing of diagnostic tests tends to avoid adsorption as immobilisation strategy, preferring complex methods that imply surface modification, covalent binding and affinity binding techniques.<sup>2-6</sup> However, for successful commercialization, antibodies need to be immobilised in bulk quantities, which needs to be achieved through a simple, reproducible and cost-effective method.<sup>2</sup> Independently of which immobilisation technique used diagnostics performance needs an antibody monolayer with controlled density, uniformity, stability and orientation for the development of sensitive and robust immunoassays.<sup>7,8</sup>

Hydrophobic substrates, such as plastics and PDMS (polydimethylsiloxane, with contact angle with water  $\sim 115^\circ$ )<sup>2,9,10</sup> are usually chosen for antibody adsorption, since hydrophobic interactions are strong enough to effectively bind an antibody to a surface.<sup>1,2,11</sup> PDMS device fabrication is, however, mainly performed by photolithography and other prototyping methods, which are difficult to upscale, since these manufacture methods do not allow mass production. Nevertheless, thermoplastic resins devices are easily mass produced by melt-extrusion or inject molding.<sup>2,8</sup> Fluoropolymers such as FEP Teflon® present excellent optical transparency that would make this substrate ideal for optical immunoassays, in addition to excellent chemical and thermal resistance, with non-reactive surfaces for a variety of chemicals and solvents. However previous adsorption studies on fluoropolymer surfaces including Teflon®<sup>12</sup> showed low levels of binding compared to e.g. gold and glass surfaces,<sup>13</sup> consistent with the 'non sticky' commercial status of fluoropolymer surfaces.

Nevertheless, our research group has recently reported unmatched levels of detection of clinically relevant biomarkers in a novel mass-manufactured fluoropolymer microfluidic material.<sup>14-17</sup> The microcapillary film (MCF) is a long ribbon made of Teflon® FEP with variable number and diameter of embedded capillaries, with contact angle with water of  $123^\circ$ .<sup>18</sup> Our previous empirical assay development studies suggested antibody adsorption into FEP Teflon® is stable, reliable, rapid and cost-effective.<sup>19-21</sup> And, although several methods for antibody covalent immobilization onto Teflon® FEP MCF have been reported, passive adsorption remains the optimal method for sensitive assays in this microfluidic platform.

1  
2  
3 which implies that antibody adsorption onto Teflon® FEP provides an uniform, strongly  
4 bound antibody monolayer with active antibodies, oriented for antigen binding.<sup>20</sup>  
5  
6 Consequently there is a need to fully understand and characterise passive adsorption of  
7  
8 diagnostics antibodies into FEP Teflon® microfluidic devices, something not reported to  
9  
10 date.

11  
12 This study shows for the first time a detailed, systematic experimental study of adsorption  
13 equilibrium and kinetics of passive antibody adsorption in actual FEP microfluidic surfaces,  
14 and the impact of FEP adsorbed antibodies on optical, enzymatic immunoassays. We  
15 explored the effect of pH, temperature and buffer concentration on antibody adsorption, also  
16 established quantitatively the effect of inner diameter of microcapillary and the link between  
17 antibody adsorption and antigen binding when the coated biosensing surface is used for  
18 heterogeneous immunoassay. Results were benchmarked against a MCF manufactured from  
19 hydrophobic LLDPE (linear low-density polyethylene) and individual glass capillaries. The  
20 low cost of MCF material means adsorption and immunoassay studies could be carried out in  
21 this study using hundreds of actual FEP microfluidic devices instead of reusing or coating a  
22 surface with a fluoropolymer layer.  
23  
24  
25  
26  
27  
28  
29  
30  
31  
32  
33

## 34 2. EXPERIMENTAL SECTION

35  
36 **2.1. Materials and Reagents.** Mouse-IgG (whole antibody) was purchased from Life  
37 Technologies (Paisley, UK), rabbit anti-mouse IgG (whole molecule) conjugated with  
38 peroxidase and SIGMAFAST™ OPD (o-Phenylenediamine dihydrochloride) tablets were  
39 supplied by Sigma-Aldrich (Dorset, UK). The BCA Protein Assay Reagent (bicinchoninic  
40 acid) was sourced from Thermo Scientific (Lutterworth, UK). The IL-1 $\beta$  recombinant  
41 protein, Anti-Human IL-1 $\beta$  biotin and Anti-Human IL-1 $\beta$  purified were supplied from  
42 eBiosciences (Hatfield, UK). High sensitivity streptavidin-HRP was supplied by Thermo  
43 Scientific (Lutterworth, UK). The Anti-troponin IgG, clone MF4 was purchased from Hytest  
44 (Turku, Finland) and the Fab specific IgG conjugated with FITC was supplied by Sigma-  
45 Aldrich (Dorset, UK).  
46  
47  
48  
49  
50  
51  
52  
53

54 Phosphate buffered solution (PBS) and Bovine Serum Albumin (BSA) were sourced from  
55 Sigma Aldrich, Dorset, UK. PBS pH 7.4, 10mM was used as the main experimental buffer.  
56 Anhydrous Sodium Carbonate was supplied from Fisher Scientific and HEPES from Sigma-  
57 Aldrich (Dorset, UK). The blocking solution consisted of 3% w/v protease-free BSA diluted  
58  
59  
60

1  
2  
3 in PBS buffer, except for IL-1 $\beta$  assays, which used a superbblocking solution supplied by  
4 ThermoScientific (Lutterworth, UK). For washings, PBS with 0.05% v/v of Tween-20  
5 (Sigma-Aldrich, Dorset, UK) was used.  
6  
7

8  
9 The 10-bore MCF material was fabricated from Teflon® FEP using a melt-extrusion process  
10 by Lamina Dielectrics Ltd. (Billingham, West Sussex, UK). The MCF used for most  
11 experiments showed a mean hydraulic diameter,  $d_h$  of  $212 \pm 16.3$   $\mu\text{m}$ , however we also tested  
12 MCFs having mean  $d_h$  of  $109 \pm 12.2$   $\mu\text{m}$  and  $375 \pm 28.6$   $\mu\text{m}$ . A 19-bore MCF materials was  
13 fabricated at Cambridge University<sup>18</sup> from LLDPE and showed a mean  $d_h \sim 200$   $\mu\text{m}$ . Single-  
14 bore glass capillaries, 152 mm in length and internal diameter of 0.58 mm were sourced from  
15 World Precision Instruments, Inc. (Hitchin, Hertfordshire, UK).  
16  
17  
18  
19  
20  
21

22 **2.2. Quantitation of antibody mass adsorbed.** The antibody mass adsorbed was quantified  
23 based on mass balance between an initial antibody solution, in a concentration range 0, 6.25,  
24 12.5, 25, 50, 100, 200 and 400  $\mu\text{g/ml}$ , and a final antibody solution obtained after 2 hour  
25 incubation in the capillaries. BCA protein assay was used for quantifying the antibody  
26 concentration in the aliquots based on solution depletion technique. Further details are  
27 provided in the supplementary information (SI) file.  
28  
29  
30  
31  
32

33 In order to understand the effect of temperature on antibody adsorption, the temperature was  
34 kept constant during IgG adsorption incubations at either 4°, 20° or 37 °C. For studying the  
35 pH effect on IgG adsorption, we prepared a IgG serial dilution in sodium carbonate buffer 10  
36 mM at pH 10.7, in Phosphate buffer (PBS) 10 mM at pH 7.4 and HEPES 10 mM at pH 4.8.  
37 The IgG solutions were incubated inside the Teflon® FEP capillaries for 2 hours at room  
38 temperature. The effect of surface chemistry on IgG adsorption was studied by comparing  
39 antibody adsorption in Teflon® FEP (Fluorinated ethylene propylene, contact angle  $123 \pm 1.6^\circ$   
40 with water)<sup>22</sup> with LLDPE (CH<sub>3</sub> plastic polymer, contact angle with water  $\sim 120^\circ$ )<sup>23</sup> and glass  
41 capillaries (borosilicate glass, with contact angle with water  $25^\circ$ )<sup>24</sup> at pH 7.4, for 2 hours at  
42 room temperature.  
43  
44  
45  
46  
47  
48  
49  
50

51 A 200  $\mu\text{g/ml}$  IgG solution dissolved in 10 mM PBS buffer pH 7.4, was incubated for 2h, at  
52 20°C in three FEP MCF with three different inner diameters: 109, 212 and 375  $\mu\text{m}$ . Protein  
53 content of the initial and final solutions was quantified by BCA method and a IgG mass  
54 adsorbed given by the protein mass balance.  
55  
56  
57

58 The adsorbed concentration, obtained from the protein mass balance before and after  
59 incubation in the capillaries, was converted to adsorbed surface density ( $\text{ng/cm}^2$ ) by dividing it  
60

by the surface area to volume ratio (SAV,  $\text{cm}^{-1}$ ), which for a circular capillary is linked to the mean  $d_h$ , (cm) of the capillary:

$$SAV = \frac{4}{d_h} \quad (1)$$

Antibody adsorption on Teflon® FEP was modelled as a Langmuir isotherm based on equation (2), best-fitted to experimental data using the minimum squares difference in Excel® solver:

$$\tau = \tau_{max} \frac{K \cdot [IgG]}{1 + K \cdot [IgG]} \quad (2)$$

where  $\tau$  is the surface coverage in equilibrium ( $\text{ng}/\text{cm}^2$ ),  $\tau_{max}$  is the number of adsorption sites available given by a maximum adsorbed concentration ( $\text{ng}/\text{cm}^2$ ),  $K$  is the adsorption constant ( $\text{ml}/\mu\text{g}$ ) and  $[IgG]$  is the antibody concentration in solution ( $\mu\text{g}/\text{ml}$ ).

**2.3. Kinetics of antibody adsorption onto different microcapillary surfaces.** Kinetic studies were also performed using the solution depletion technique and calculating the mass balance between initial antibody concentration and after variable incubation times in the capillaries; for details are provided in SI file.

The kinetics of antibody adsorption kinetics were assumed to follow equation 3, fitted to experimental data based on minimum squares difference. This equation is the algebraic solution of a differential equation given by the difference between the adsorption and desorption processes of the reactant to free binding sites:

$$\tau(t) = \frac{K_{on} [IgG]}{k_{on} [IgG] + K_{off}} [1 - \exp [ - (K_{on}[IgG] + K_{off}) \cdot t]] \quad (3)$$

where  $\tau(t)$  is the surface coverage ( $\text{ng}/\text{cm}^2$ ) at a given experimental time,  $t$  (min),  $[IgG]$  is the antibody bulk concentration (M),  $K_{on}$  is the adsorption rate ( $\text{M}^{-1} \text{min}^{-1}$ ) and  $K_{off}$  is the desorption rate ( $\text{min}^{-1}$ ).



1  
2  
3 For simplicity, kinetic adsorption data has been presented as percentage surface coverage,  $\phi$   
4 computed by normalising  $\tau$  with the theoretical antibody monolayer assuming vertical  
5 antibody orientation based on a reference dimensions for an antibody molecule  
6 (14.2nm $\times$ 8.5nm $\times$ 3.8nm)<sup>25</sup>. In order to account for different sizes of microcapillaries and  
7 enable direct comparison of different capillary systems, the percentage  $\phi$  was further  
8 normalised by SAV described in equation 1.  
9  
10  
11  
12  
13

14 **2.4. Effect of buffer ionic strength in antibody adsorption onto Teflon® FEP by confocal**  
15 **microscopy.** In this study 25 and 50  $\mu$ g/ml solutions of anti-TnI were prepared in different  
16 concentrations of PBS buffer at pH 7.4: 0.625, 1.25, 2.5, 5 and 10 mM. The 10 solutions were  
17 aspirated into 8 MCF strips, each 8 cm in length, and incubated for 2 hours. After a blocking  
18 step, Fab specific IgG conjugated with FITC was incubated, followed by a final washing. The  
19 strips were inserted into a MCF holder<sup>17</sup> and imaged with a confocal microscope (LSCM,  
20 Nikon inverted Microscope ECLIPSE TE300 with Bio-Rad RAD200, scan head 60X-1.20NA  
21 objective lenses, excitation peak wavelength of 488 nm and emission peak wavelength of  
22 530 nm, operating Laser Sharp 2000 software). Fluorescence images were then analysed with  
23 ImageJ software (NIH, USA), splitting the RGB image, and using the green channel to  
24 produce a greyscale plot, where the height of fluorescent peak was considered the fluorescent  
25 intensity.  
26  
27  
28  
29  
30  
31  
32  
33  
34

35 **2.5. Quantitation of antibody adsorbed onto Teflon® FEP using polyclonal mouse-**  
36 **IgG/anti-mouse IgG ELISA.** To study the effect of immobilised antibody density in  
37 antibody binding in an assay (i.e. capacity of a coated solid phase to specifically capture  
38 molecules), a total of 8 Teflon® FEP MCF strips were incubated for 2 hours at room  
39 temperature with 0, 6.25, 12.5, 25, 50, 100, 200 and 400  $\mu$ g/ml of mouse IgG in PBS 10 mM,  
40 pH 7.4. The strips were then washed and non-specific surface sites blocked. Three different  
41 concentrations of anti-IgG polyclonal conjugated to peroxidase (60, 600, 6000  $\mu$ g/ml) were  
42 added and incubated for 10 minutes. After a washing step the OPD enzymatic substrate was  
43 added and images were taken with a flatbed scanner. More details are provided in SI file.  
44  
45  
46  
47  
48  
49  
50

51 In order to understand the effect of surface area available, this experiment was repeated using  
52 600 ng/ml of anti-IgG conjugated with peroxidase in different bore MCFs of 109  $\mu$ m and 375  
53  $\mu$ m. Note that in this method of quantitation the ELISA returned an optical signal that cannot  
54 be converted to surface coverage, therefore the relative antibody adsorption was modelled  
55  
56  
57  
58  
59  
60

1  
2  
3 based on absorbance values and a modified Langmuir isotherm detailed in supporting  
4 material.  
5

6  
7 The effect of immobilised IgG incubation time in antibody binding was studied by incubating  
8 40  $\mu\text{g/ml}$  of IgG in PBS in Teflon® FEP MCF strips from 0 to 120 minutes, before washing  
9 the strips with 1 ml PBS-Tween. A solution of 600  $\text{ng/ml}$  of anti-IgG, peroxidase conjugated  
10 was then added and incubated for 10 minutes. After another washing step, OPD enzymatic  
11 substrate was added at the concentration of 1  $\text{mg/ml}$ . The MCF strips were then imaged after  
12 5 minutes incubation of OPD in transmittance mode.  
13  
14  
15  
16  
17

18 **2.6. IL-1 $\beta$  sandwich ELISA using monoclonal antibodies.** In order to determine the  
19 optimum antibody surface coverage for a monoclonal antibody system, 6 cm long Teflon®  
20 FEP MCF strips were filled with IL-1 $\beta$  monoclonal antibody solutions of 20, 40, 100 and 140  
21  $\mu\text{g/ml}$  and incubated for 2 hours. Further steps involving surface blocking, washing,  
22 incubation of 0.5  $\text{ng/ml}$  of recombinant IL-1 $\beta$ , addition of IL-1 $\beta$  biotinylated antibody and  
23 High Sensitivity Streptavidin-HRP with OPD enzymatic substrate were followed with final  
24 MCF strips images taken with a Flatbed Scanner at 2400 dpi. Further details are provided in  
25 SI.  
26  
27  
28  
29  
30  
31

32 For the IL-1 $\beta$  response curves, three 30 cm long Teflon® FEP MCF strips were filled with 40  
33  $\mu\text{g/ml}$  of IL-1 $\beta$  capture antibody (capAb). One of the strips was incubated for 30 minutes and  
34 the other two for 2 hours. The strips underwent blocking, washing, incubation of eight  
35 solutions of IL-1 $\beta$  from 0 to 1  $\text{ng/ml}$ , addition of IL-1 $\beta$  biotinylated antibody followed by a  
36 wash step and high sensitivity streptavidin-HRP and OPD enzymatic substrate incubation.  
37 The MCF strips were imaged by a Flatbed Scanner.  
38  
39  
40  
41  
42  
43

44 **2.7. Image Analysis of MCF ELISA strips.** RGB digital images were split into 3 separated  
45 channels in Image J (NIH, USA). The blue channel images were used to calculate absorbance  
46 values, based on the grey scale peak height of each individual capillary of Teflon® FEP MCF  
47 as described elsewhere.<sup>16,21</sup> Further details about image analysis procedure are provided in SI.  
48  
49

50 2.3. Kinetics of antibody adsorption onto different microcapillary surfaces.  
51

## 52 **3. RESULTS AND DISCUSSION**

### 53 **3.1. Effect of temperature, pH and buffer ionic strength on adsorption equilibrium.**

54 Conventionally, the driving force for protein adsorption is regarded as an entropy gain arising  
55 from the release of surface adsorbed water molecules and salt ions and from structural  
56 rearrangements inside the protein,<sup>26</sup> therefore the first set of experiments aimed at exploring  
57  
58  
59  
60

1  
2  
3 the effect of temperature, pH and buffer ionic strength on antibody adsorption equilibrium for  
4 the 10-bore, Teflon® FEP MCF strips containing microcapillaries with mean  $d_h$  of 212  $\mu\text{m}$ ,  
5 using mouse IgG as a model.  
6  
7

8  
9 Surprisingly, the effect of temperature was found negligible in respect to the mass of IgG  
10 adsorbed as shown by the Langmuir isotherms shown in Figure 1A and best-fitted Langmuir  
11 model parameters summarised in Table 1. Values of  $\tau_{max}$  and  $K$  (equation (2), for 10mM PBS  
12 and pH 7.4) varied less than 2% and 7%, respectively, for the range of temperatures tested (4,  
13 20 and 37 °C), with an average value of  $\tau_{max} = 476 \text{ ng/cm}^2$ , which contradicts the temperature  
14 enhancement of protein adsorption reported in literature for other biosensing surfaces,<sup>1,11,27</sup>  
15 however in alignment with protein adsorption studies on hydrophobic surfaces. As FEP is  
16 substantially hydrophobic<sup>28</sup> (i.e. water repellent) our results suggest passive adsorption of  
17 IgG molecules to FEP is connected to the rate of release of water molecules which remained  
18 constant for the range of temperatures tested. Chen et al.<sup>29</sup> showed the number of water  
19 molecules released from the protein-adsorbent binding process remains approximately  
20 constant for temperatures below 40 °C. Also, the same study showed the binding affinity of  
21 protein adsorption to hydrophobic surfaces remained almost unchanged at temperatures  
22 below 40 °C due to proteins maintaining the original protein conformation at such  
23 temperatures. Although extensive literature has identified enthalpy and entropy effects in  
24 hydrophobic interaction systems, it appears protein adsorption to FEP at these temperatures  
25 follows a simple monolayer adsorption behaviour. This represents an advantage in respect to  
26 manufacturing of FEP microfluidic biosensing devices, as it removes the need of precise  
27 temperature control, lowering the cost of manufacturing and enabling a higher degree of  
28 freedom to operators.  
29  
30  
31  
32  
33  
34  
35  
36  
37  
38  
39  
40  
41  
42  
43

44 Reduction in pH below the isoelectric point (typically 6.3-8.9 for IgG<sup>30</sup>) resulted on an  
45 increase to the amount of IgG adsorbed onto Teflon® FEP microcapillaries (Figure 1B), with  
46  $\tau_{max}$  increasing by 76%, from 484 to 853  $\text{ng/cm}^2$  (Table 1) whereas an increase in pH to 10.7  
47 resulted on a 58% decrease to  $\tau_{max}$  down to  $\sim 200 \text{ ng/cm}^2$ . Conventionally, adsorption rates are  
48 higher when protein and substrate bear opposite charges, since electrostatic attractions  
49 accelerate the migration towards the surface<sup>1,31</sup>, consequently the Langmuir isotherm plots in  
50 Figure 1B suggested at first sight that FEP is negatively charged (which is the case for some  
51 FEP resins available in the market), however the rate of adsorption equilibrium constant,  $K$ ,  
52 in FEP microcapillaries was smaller at lower pH, meaning no charge difference between the  
53 surface and the IgG molecules. This increase in mass of antibody adsorbed at lower pH  
54  
55  
56  
57  
58  
59  
60

(Table 1) can instead be explained by protein denaturation, which promotes unfolding and aggregation of antibody molecules, in line with the works of e.g. Wright and co-authors<sup>32</sup> reported about 50% of the antibody denatured in solution at pH 4.95.

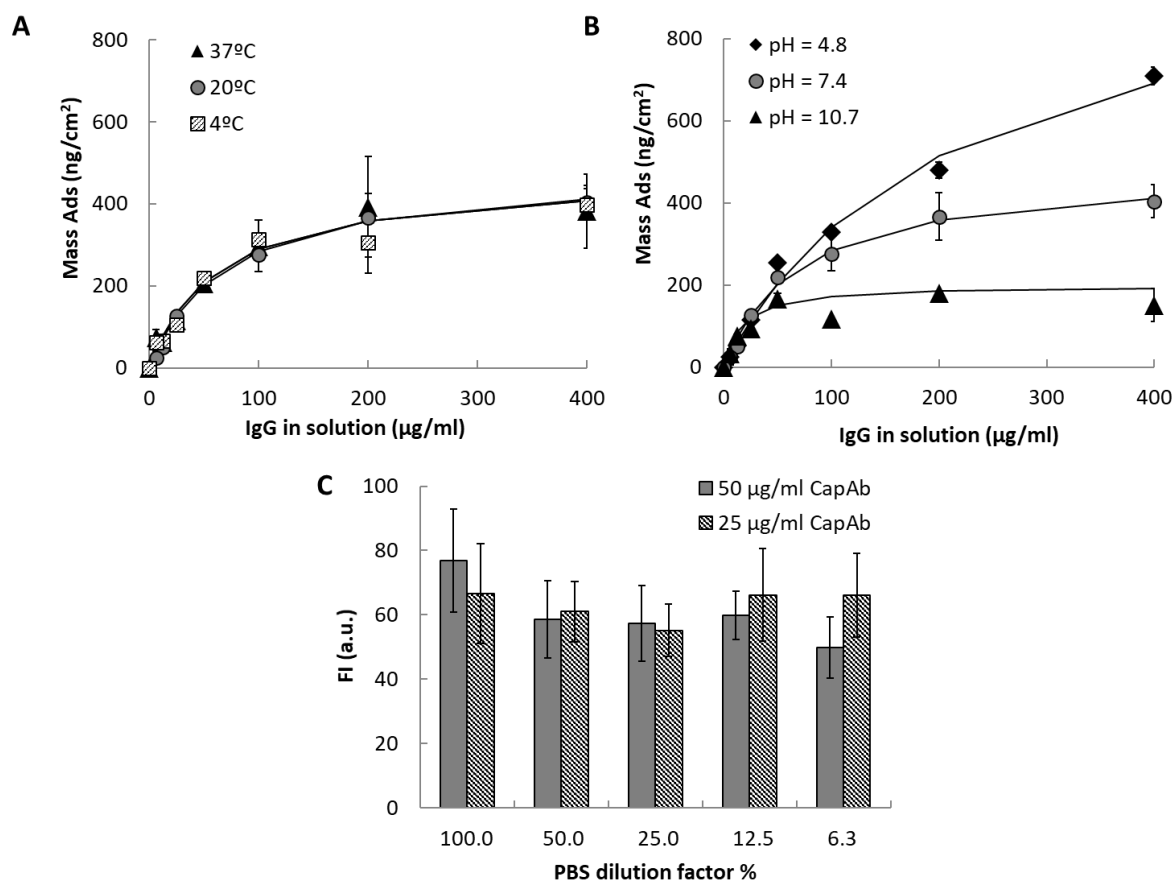


**Figure 1.** Effect of temperature, pH and buffer concentration on adsorption of mouse IgG on 10-bore, Teflon® FEP MCF strips having mean  $d_h$  of 212  $\mu\text{m}$ . **A** Adsorption isotherms at 4, 20 and 37 °C (constant pH 7.4). **B** Antibody adsorption isotherms at pH 4.8, 7.4 and 10.7 (constant temperature 20 °C). **C** Effect of buffer dilution on antibody adsorption, as recorded with fluorescence confocal microscopy. Note that initial PBS solution contains 10 mM phosphate buffer, 2.7 mM potassium chloride and 137 mM sodium chloride. The continuous lines in A and B represent the best-fitted Langmuir isotherms with parameters summarised in Table 1.

The Langmuir plots shown in Figure 1B suggested adsorption of IgG in FEP microcapillaries was most effective at a pH closest to the isoelectric point of IgG, where electrostatic protein–

protein repulsions are minimized and higher packing densities possible on the FEP surface. This agrees with our vast experience in immunoassays development in the FEP microcapillaries, with ideal pH for immunoassays always around the isoelectric point, see for example Barbosa *et al.*<sup>14,16</sup> and Castanheira *et al.*<sup>15</sup>

We also noticed the concentration of dissolved ions (also known as ionic strength) in the bulk antibody solution had negligible effect on the amount of immobilized antibody (Figure 1C). There was no significant change in the fluorescent signal used to identify immobilised antibody layers dissolved PBS buffer at different dilution ratios, yielding a range of 0.6-10mM for phosphate, 0.3-2.7 mM potassium chloride and 17.1-137 mM sodium chloride (Figure 1C). It has been reported previously that increased salt concentrations reduce electrostatic repulsion between like-charged material, favouring IgG adsorption, and decreases electrostatic attraction between oppositely charged material, impeding adsorption.<sup>33</sup> Consequently, these new results suggest antibody adsorption onto Teflon® FEP is driven by hydrophobicity not by electrostatic interactions. A previous study of protein adsorption on silicon surfaces by Zhao *et al.*<sup>34</sup> reported a reduction on antibody adsorption only for very high salt concentrations of 150 mM and above, at lower salt concentration antibody adsorption remained very consistent. Our data shows no difference in antibody adsorption to FEP microcapillaries up to 137 mM of sodium chloride, 2.7 of potassium chloride and 10 mM of phosphate buffer, which suggests antibody adsorption to Teflon® FEP is stable even for high salt concentrations (Figure 1C).

**Table 1.** Best-fitted parameters for Langmuir isotherms (based on equation 2 and plotted in Figure 2) describing antibody adsorption in Teflon® FEP microcapillaries at varying pH and temperatures.

	Temperature			pH		
	4°C	20°C	37 °C	4.8	7.4	10.7
<b><i>K</i> (ml/μg)</b>	0.015	0.014	0.016	0.007	0.014	0.061
<b><i>τ</i><sub>max</sub> (ng/cm<sup>2</sup>)</b>	472	484	472	853	484	200
<b>R<sup>2</sup></b>	0.9856	0.9963	0.9891	0.9801	0.9963	0.9413

On the overall, the optimal adsorption conditions shown in Figure 1 revealed a surface density of antibody onto Teflon® FEP microcapillaries of ~400 ng/cm<sup>2</sup> when coated with 400 μg/ml of IgG in bulk solution. This yields a “loading density” of ~2,000 ng/cm<sup>2</sup>, calculated by dividing the loaded antibody concentration by the SAV (Equation 1). This ~5-fold excess

of antibody required to fully coat the plastic surface is evidence of low affinity for adsorption of IgG to the Teflon® FEP surface, which is also confirmed by the reduced adsorption constant of 0.014 ml/μg (Table 1). This suggests at first sight that antibody immobilisation onto FEP and other fluoropolymer surfaces is very inefficient, nevertheless the mass adsorbed onto FEP microcapillaries was found very similar to values reported to other hydrophobic and fluorinated surfaces at similar physical conditions. For example, a IgG adsorption study on gold electrodes coated with Teflon AF (amorphous fluoropolymers) based on optical waveguide light mode spectroscopy<sup>35</sup> reported a surface density of approximately 200 ng/cm<sup>2</sup>, similar to the 220 ng/cm<sup>2</sup> obtained in our Teflon® FEP microcapillaries, both using 40 μg/ml of IgG in bulk solution. Another study by Wiseman and Frank<sup>36</sup> based on quartz crystal microbalance with dissipation in a CH<sub>3</sub>-terminated surface (1-dodecanethiol self-assembled monolayer on gold) reported a maximum coverage of 468 ng/cm<sup>2</sup> with 100 μg/ml IgG in solution. This value was ~40% larger than the surface coverage obtained with our 10-bore, 212 μm Teflon® FEP MCF (275 ng/cm<sup>2</sup>) using the same IgG concentration. This difference might be due either to the differences in geometry and/or surface chemistry. In spite of a lower ‘affinity’ to antibody adsorption, Teflon® FEP is not less effective than other surfaces for immobilising proteins and in particular IgG antibody molecules.

### 3.2. Impact of capillary diameter and surface coverage on antibody-antigen

**equilibrium.** A key parameter able to dictate the fate of an heterogeneous immunoassay, perhaps even more relevant than the total mass of antibody adsorbed, is the amount of antibody than is readily available to bind the antigen or secondary reagents. Consequently we characterised the impact of antibody adsorption and surface coverage on immune-binding of a targeted protein using a labelled secondary antibody.<sup>13</sup> This is an essential feature for successful use of FEP microfluidic surfaces in actual immunoassays, such as colourimetric or fluorescent ELISA. Whenever performing this methodology it is paramount to understand the effect of labelled antibody bulk concentration (that acts as an antigen) in the equilibrium as illustrated in Figure 2A.

As expected, an increase in surface density of adsorbed mouse IgG (computed from the coating antibody concentration and adsorption plots shown in Figure 1) led to an increase on optical signal, meaning a higher extent of binding of adsorbed antibody with the labelled anti-mouse IgG (acting as Ag). We tested 212 μm i.d. Teflon® FEP microcapillaries with concentrations of Ag covering three orders of magnitude, being 60, 600 and 6,000 ng/ml of

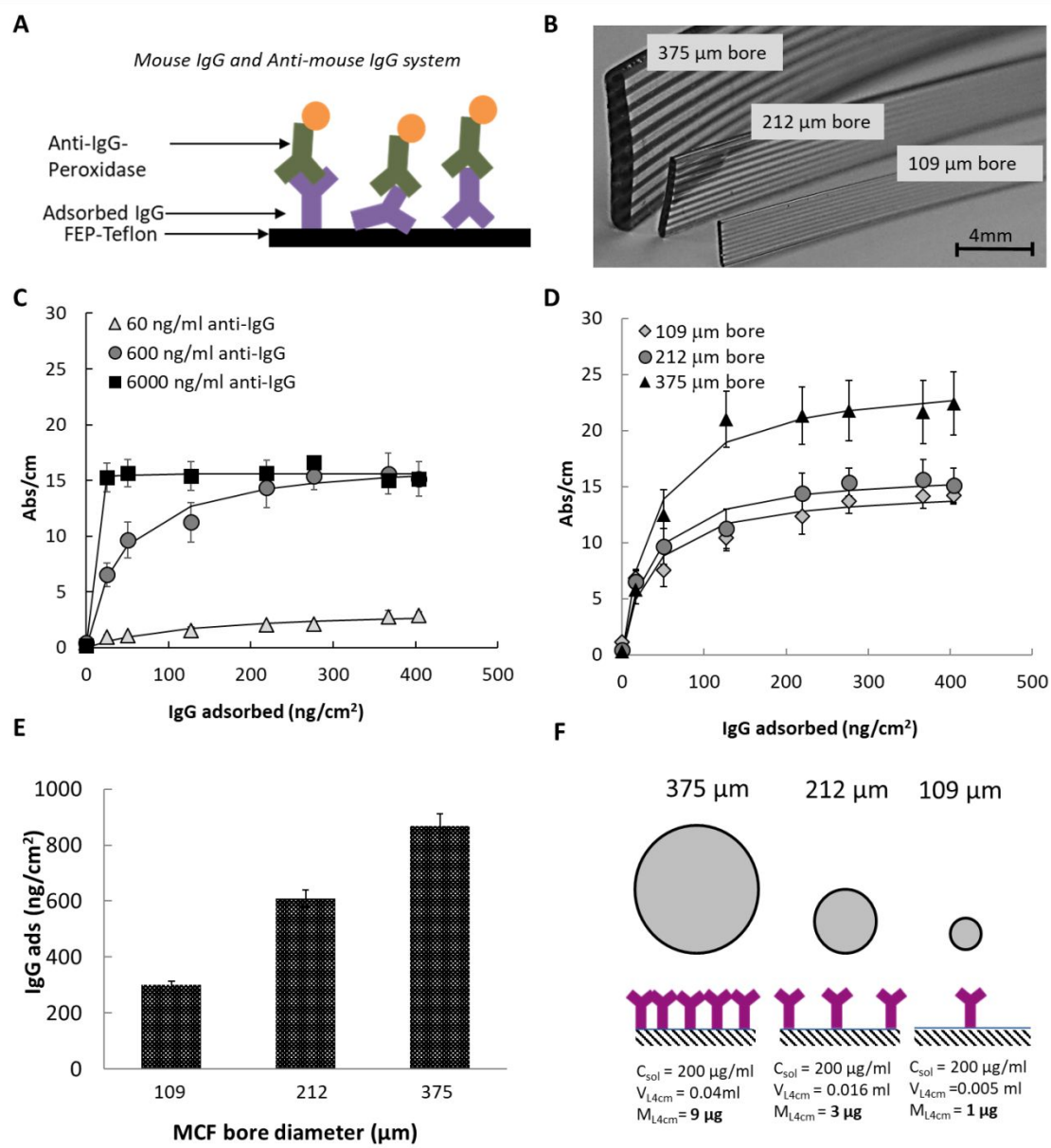


**Figure 2.** Effect of antibody surface coverage in antibody-antigen binding on Teflon® FEP MCF using a polyclonal, mouse IgG/anti-mouse IgG system. **A** Schematic diagram of direct ELISA with anti-mouse IgG conjugated to peroxidase (“antigen”) binding to immobilised mouse-IgG antibody. **B** Microphotograph of 10-bore Teflon® FEP MCFs having different bore sizes:  $109 \pm 12.2 \mu\text{m}$ ,  $212 \pm 16.3 \mu\text{m}$  and  $375 \pm 28.6 \mu\text{m}$ . **C** Effect of antibody surface coverage on optical immunoassay signal in the  $212 \mu\text{m}$  mean  $d_h$  FEP MCF with different concentrations of anti-mouse IgG. **D** Effect of internal diameter of FEP microcapillary and antibody surface coverage on optical immunoassay signal for a fixed concentration of anti-mouse IgG. The continuous lines in C and D show the best-fitted Langmuir isotherms with parameters summarised in Tables S1 and S2. **E** Antibody mass adsorbed on FEP

1  
2  
3 microcapillaries with 109, 212 and 375  $\mu\text{m}$  inner bore diameter. **F** Schematic diagram  
4 explaining the relation between microcapillary bore diameter and antibody adsorption.  
5  
6  
7  
8

9 anti-mouse IgG. At the highest concentration of anti-mouse IgG, a small density of IgG  
10 adsorbed of 20-40  $\text{ng}/\text{cm}^2$  revealed sufficient to saturate the optical signal (Figure 2C). At  
11 lower concentrations there was a clear correlation between the surface density of adsorbed  
12 IgG and the optical signal (Figure 2C), and followed a typical Langmuir isotherm has shown  
13 in Table S1 (see SI file). Note these experiments cannot provide information about antibody  
14 orientation as the selected labelled non-specific anti-mouse IgG is able to bind any part of the  
15 immobilized IgG antibody, however these provide essential evidence regarding the  
16 importance of the labelled antibody (anti-IgG) concentration and immobilized antibody  
17 surface coverage in the binding equilibrium.  
18  
19  
20  
21  
22  
23  
24

25 Additionally, we explored the effect of inner capillary diameter by testing MCF strips with  
26 three different inner diameters (Figure 2B) and noticed optical immunoassay signal increased  
27 with increasing inner diameters of the FEP microcapillaries. This is also shown by the  
28 increasing  $Abs_{max}$  values in Table S2 (see SI file). This results from the fact larger capillaries  
29 present a larger surface area for adsorbing the capAb, therefore yielding higher antibody  
30 surface coverage (Figures 2D-F) which favours antigen binding in an actual immunoassay.  
31 The optical signal obtained with 600  $\text{ng}/\text{ml}$  anti-IgG was >60% larger in the 375  $\mu\text{m}$  i.d.  
32 microcapillary compared to the 212  $\mu\text{m}$  i.d. microcapillary, suggesting antibody adsorption is  
33 also very dependent on the geometry of the biosensing surface in addition to the surface  
34 chemistry (this is further described later in this manuscript). Higher antibody surface  
35 coverage for larger inner diameter capillaries was also determined through the IgG mass  
36 balance (Figure 2E) confirming the dependency of adsorbed antibody density and inner  
37 diameter of FEP microcapillaries. This is to our knowledge the first time this diameter effect  
38 has been reported in literature and it might be due to a fact unique to cylindrical  
39 microcapillaries, enabling to coat the whole cross section with the antibody/protein, in  
40 contrast to conventional microchannel-based devices.  
41  
42  
43  
44  
45  
46  
47  
48  
49  
50  
51  
52  
53

54 **3.3. Effect of antibody surface coverage on antibody activity and orientation.** We studied  
55 the link between adsorbed antibody surface coverage and antibody activity and orientation in  
56 FEP microcapillaries by performing a sandwich ELISA with adsorbed monoclonal  
57  
58  
59  
60



antibodies, capable of uniquely binding to a specific epitope in an antigen molecule (Figure 3A).

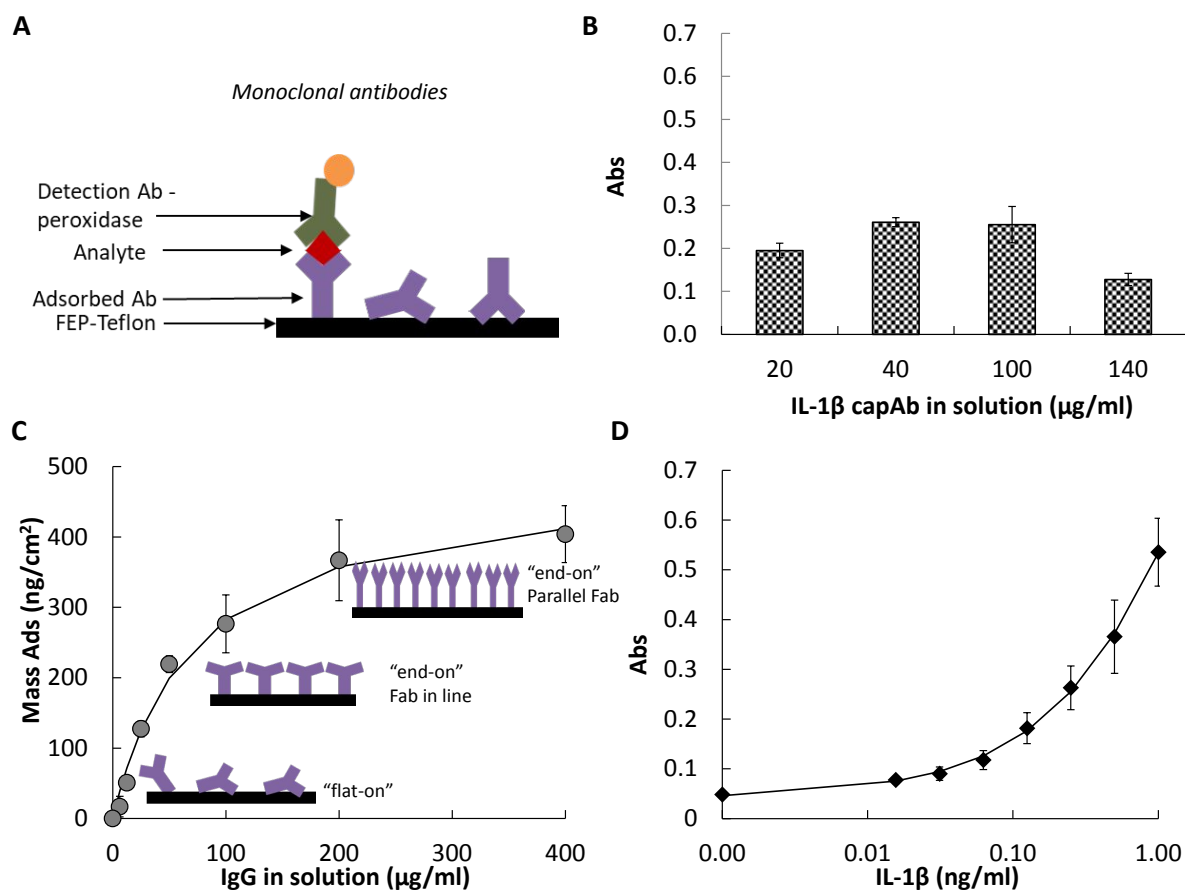


**Figure 3.** Effect of antibody surface coverage in antibody activity/orientation on 212 μm Teflon® FEP MCF. **A** Schematic diagram of sandwich ELISA based on adsorbed monoclonal capAb and monoclonal detection antibody directly conjugated to peroxidase. **B** Effect of concentration of capAb coating on optical signal, showing antibody surface coverage influences antibody activity/orientation in FEP microcapillaries. **C** Antibody adsorption isotherm at 20°C, pH 7.4 and 10mM of PBS, with the continuous line representing the best-fitted Langmuir model (Equation 2), with best-fitting parameters summarised in Table 2, along with schematic representation of hypothesized relation between surface coverage and antibody orientation on Teflon®FEP, supported by experimental data and literature. **D** Full response curve for quantitation of IL-1β, showing optical quantitation of clinically relevant biomarkers is feasible based on passive antibody adsorption in fluoropolymer microfluidic devices.

1  
2  
3  
4  
5  
6  
7  
8  
9  
10  
11  
12  
13  
14  
15  
16  
17  
18  
19  
20  
21  
22  
23  
24  
25  
26  
27  
28  
29  
30  
31  
32  
33  
34  
35  
36  
37  
38  
39  
40  
41  
42  
43  
44  
45  
46  
47  
48  
49  
50  
51  
52  
53  
54  
55  
56  
57  
58  
59  
60

Contrary to the polyclonal system, as the binding region needs to be available within an intact protein structure, a drop on the optical signal in the sandwich immunoassay (schematically summarised in Figure 3A) evidenced denaturation and/or inadequate orientation of capAb during adsorption but also steric hindrance caused by neighbour adsorbed antibodies. Antibody surface coverage and antibody activity are major aspects in consideration for the development of any high-performance immunoassay tests, such as those aimed at cardiovascular diseases and cancer diagnosis, and this has not been studied to date for fluoropolymer surfaces.

In contrast to the polyclonal system discussed previously, we observed a rapid drop in optical signal with the increase in concentration of capAb above the window 40-100  $\mu\text{g/ml}$  (Figure 3B). Note this data was gathered using 0.5 ng/ml of IL-1 $\beta$  antigen, it is likely the threshold will depend on the antibody pair but also on the limit of detection and cut-off aimed for the antigen. The antibody densities estimated with Langmuir model were 175 ng/cm<sup>2</sup> for 40  $\mu\text{g/ml}$  of antibody in solution and 277 ng/cm<sup>2</sup> with 100  $\mu\text{g/ml}$  corresponding, respectively, to 45% and 69% of the maximum total mass adsorbed onto Teflon® FEP capillaries, based on a theoretical antibody monolayer estimated as 440 ng/cm<sup>2</sup>, assuming an antibody size of 14.2nm $\times$ 8.5nm $\times$ 3.8nm.<sup>25</sup> This suggests the adsorbed antibody achieved the maximum capacity to bind the antigen within less than full monolayer, which is commensurate with data reported in literature for other immunoassay surfaces.<sup>37</sup>

The combined analysis of experimental data gathered with distinct methodologies (i.e. protein mass titration summarised in Figure 1, and optical ELISAs using monoclonal and polyclonal antibodies summarised in Figures 2 and 3, suggested surface coverage density is directly linked to antibody orientation and binding capacity of Teflon® FEP capillaries schematically represented in Figure 3C. We hypothesised that lower antibody surface densities favour antibodies adsorbed on “flat on” orientation (both Fc and Fab fragments adsorbed onto the surface) whereas large antibody densities favour “end on” orientation, with Fab region towards the solution (Figure 3C). This hypothesis is supported by current literature. Firstly, based on the dimensions of antibody molecules, Buijs and co-authors<sup>38</sup> suggested a relationship between the mass adsorbed and the orientation of the molecule on the surface, with 200 ng/cm<sup>2</sup> representing a monolayer with antibodies in a “flat-on” orientation, 260 ng/cm<sup>2</sup> in an “end on” orientation with Fab fragments in line, and 550 ng/cm<sup>2</sup> in an “end-on” orientation with Fab fragments close together and parallel, which

1  
2  
3 explains reduced activity of adsorbed antibody due to the proximity of Fab fragments. This  
4 suggests antibody adsorption onto Teflon® FEP at the conditions studied happened through a  
5 monolayer formation with the maximum adsorbed amount of approximately 404 ng/cm<sup>2</sup>,  
6 which suggests a packed antibody monolayer with antibodies oriented “end-on” with Fab  
7 fragments in line with Buijs and co-authors<sup>38</sup>, based on a theoretical monolayer for  
8 Teflon@FEP of ~440 ng/cm<sup>2</sup>. Other studies reported antibody denaturation of the Fab region  
9 with loss of antibody binding capacity to Teflon surfaces,<sup>39,40</sup> however those findings are not  
10 supported by the data presented in this study. The optical sandwich ELISA based on adsorbed  
11 antibody yielded a good limit of detection (23 pg/ml or 0.74 pM of IL-1β), for antibody  
12 surface coverage of 175 ng/cm<sup>2</sup> (Figure 3D), comparable to gold-standard microtiter plate  
13 based ELISA. This confirms again that antibodies adsorbed in Teflon@FEP assume an “end-  
14 on” position, available for antigen binding from 45% to 69% of an antibody monolayer, as  
15 previously discussed for Figure 3B, which approaches the values proposed by Buijs and co-  
16 authors<sup>38</sup>. Xu and co-authors<sup>41</sup> reported a similar relationship with hydrophilic silicon oxide.  
17 Zhao and co-authors<sup>34</sup> reported that the binding capacity of an immobilised antibody is  
18 greater for surface coverages below 50% of full monolayer, above this threshold the binding  
19 sites in the antibody molecules can become inaccessible to the antigen. Also, higher antibody  
20 densities decreases the degree of irreversibility of antibodies bond to the surface, with the  
21 irreversibly adsorbed amount being a maximum 250 ng/cm<sup>2</sup> on a hydrophilic silicon oxide  
22 surface.<sup>41</sup>

23  
24  
25  
26  
27  
28  
29  
30  
31  
32  
33  
34  
35  
36  
37  
38 Further studies support the relationship between surface coverage and antibody  
39 orientation/binding capacity and the hypothesis for antibody adsorption onto Teflon@FEP.  
40 The work of Wiseman and co-authors<sup>42</sup> based on quartz crystal microbalance with  
41 dissipation, detected a shift in dissipation value of the crystal almost to zero for a mass of  
42 antibody adsorbed below 200 ng/cm<sup>2</sup>, meaning that this initial mass is strongly attached to  
43 the surface and suggesting “flat-on” orientation of the antibody. Neutron reflexion studies by  
44 Xu and co-authors<sup>41</sup> revealed a 4 nm thick layer, which is close to the short axial length of an  
45 antibody molecule, for a mass adsorbed of 220 ng/cm<sup>2</sup>, also suggesting a “flat-on”  
46 orientation. Above 200 ng/cm<sup>2</sup> both Wiseman and co-authors<sup>42</sup> and Xu and co-authors<sup>41</sup>  
47 showed an increase on dissipation slope, meaning new antibodies are adsorbed onto the  
48 surface in a less rigid mechanical coupling, suggesting “end-on” orientation of molecules.  
49 Surprisingly, Wiseman and co-authors<sup>42</sup> reported no decrease in antibody binding capacity  
50 with surface densities above 50% of the monolayer, suggesting an active antibody monolayer  
51  
52  
53  
54  
55  
56  
57  
58  
59  
60

1  
2  
3 is achieved at  $\sim 468$  ng/cm<sup>2</sup>. A further increment in bulk IgG concentration resulted in higher  
4  
5 dissipation values, suggesting a multilayer formation.<sup>36</sup>  
6

7  
8 On the overall, the sandwich ELISA with monoclonal antibodies confirmed that antibodies  
9  
10 adsorb onto FEP just like other surfaces with good stability and activity, in contrast to what  
11  
12 has been suggested by few previous publications in hydrophobic Teflon® surfaces.<sup>39,40</sup> This  
13  
14 is probably linked to the fact that we used actual, unmodified fluoropolymer surfaces,  
15  
16 whereas previous studies were based on glass surface coated with Teflon or even on latex  
17  
18 suspensions as the case of Vermeer and co-authors<sup>39,40</sup> (they used Teflon particles with mean  
19  
20 diameter 215 nm), which clearly was insufficient to mimic the real chemistry of  
21  
22 fluoropolymer surface.

23  
24 **3.4. Kinetics of adsorption of IgG antibody for FEP.** In addition to equilibrium adsorption  
25  
26 isotherms, we have also studied the kinetics of IgG adsorption onto fluoropolymer  
27  
28 microcapillary surfaces, this is important to inform the on/off rates of immobilised antibodies  
29  
30 and the time required to manufacture MCF diagnostic strips, impacting on the throughput and  
31  
32 consequently the final cost of the tests. Adsorption kinetics can also inform about the strength  
33  
34 of the bond with the plastic substrate (surface), degree of reversible antibody adsorption or  
35  
36 antibody denaturation, and modifications in the binding capacity of the adsorbed antibody.

37  
38 We noticed adsorption of IgG onto Teflon® FEP was surprisingly fast, with equilibrium  
39  
40 reached within 5-10 minutes and independent of the concentration of IgG loaded into the  
41  
42 microcapillaries. This was unequivocally shown in data collected by both the solution  
43  
44 depletion technical (Figure 4A) and ELISA (Figure 4B), the two data sets are further  
45  
46 compared in Figure 4C in terms of normalised signal, being 100% the mean value at plateau.  
47  
48 We estimated  $K_{on}$  in order of  $10^5$  M<sup>-1</sup>min<sup>-1</sup> at small bulk concentrations (20 and 40  $\mu$ g/ml) and  
49  
50 in the order of  $10^6$  M<sup>-1</sup>min<sup>-1</sup> for larger antibody bulk concentrations (200  $\mu$ g/ml) as  
51  
52 summarised in Table 2. The percentage surface coverage  $\phi$  summarised in Figure 4B was  
53  
54 computed based on a full theoretical monolayer with all antibodies in the “end on” position.  
55  
56 Two full IL-1 $\beta$  response curves made with 30 minutes and 120 minutes of monoclonal  
57  
58 antibody adsorption, revealed lower limits of detection of 61 pg/ml (1.97 pM) and 54 pg/ml  
59  
60 (1.75 pM) respectively (Figure 4D), which shows that between 30 to 120 minutes of  
adsorption onto Teflon@FEP, antibody binding capacity is not significantly affected.

**3.5. Effect of surface chemistry in antibody surface coverage and adsorption kinetics.**

Surface chemistry is by far identified in literature as the main factor influencing antibody

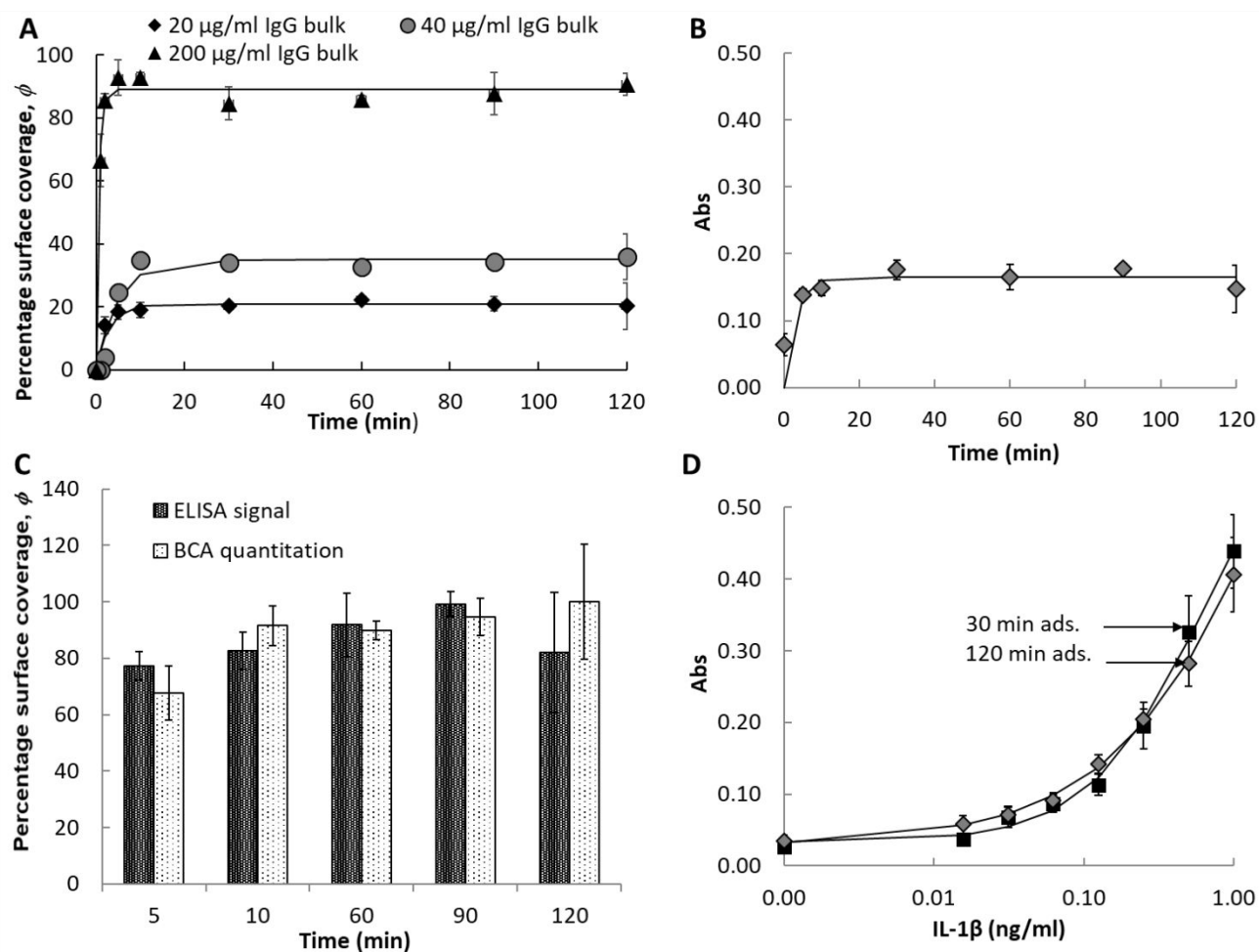


**Figure 4.** Kinetics of antibody adsorption in Teflon® FEP microcapillaries having mean  $d_h$  of 212  $\mu\text{m}$ . **A** Mass of antibody adsorbed expressed in terms of percentage of surface coverage,  $\phi$  using increasing times of incubation of mouse IgG concentrations of 20, 40 and 200  $\mu\text{g/ml}$  (corresponding to  $1.3 \times 10^{-7}$  M,  $2.6 \times 10^{-7}$  M and  $1.3 \times 10^{-6}$  M, respectively), determined by solution depletion technique. **B** Kinetics of generation of optical signal measured by ELISA based on 40  $\mu\text{g/ml}$  of mouse-IgG coating at varying times and 600 ng/ml of anti-mouse IgG conjugated to peroxidase. **C** Direct comparison of mouse-IgG antibody quantitation by BCA assay shown in A with optical ELISA in mouse-IgG/anti-mouse IgG system shown in B signal, showing magnitude of optical ELISA signal is linked to mass of antibody adsorbed. **D** IL-1 $\beta$  full response curves using 40  $\mu\text{g/ml}$  of capAb incubated for 30 and 120 minutes, confirming antibody adsorption is rapid. The continuous lines in A and B represent the kinetic model based on equation 3, with best-fitted parameters summarised in Table 2. The continuous line in D represents the values obtained by the four parameter logistic (4PL) model, commonly used for full responses in immunoassays.

adsorption, therefore we have directly compared antibody adsorption with two other capillary surfaces, being a 19-bore MCF melt-extruded from LLDPE and a single-bore glass capillary (Figure 5A). As the three capillary systems presented different diameters, all adsorption data shown in this section has been normalised in respect to SAV ratio (shown in Equation 1).

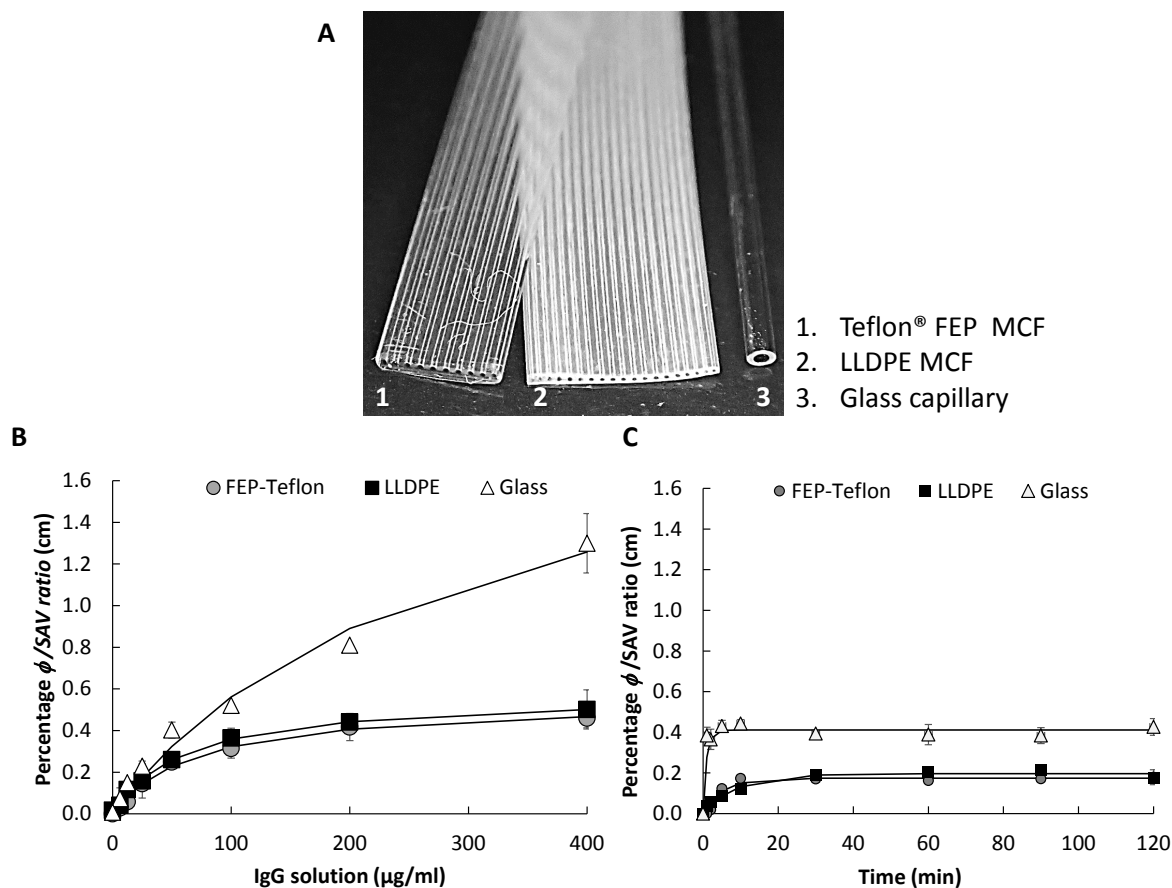


**Figure 5.** Antibody adsorption onto different capillary surfaces. **A** Microphotograph of capillary systems tested in this study, being: 1 - 10 bore Teflon® FEP MCF, 2 – 19 bore LLDPE MCF, 3 – single-bore glass capillary. **B** Antibody adsorption isotherms expressed as percentage surface coverage,  $\phi$  to SAV ratio ( $\text{cm}^{-1}$ ) of IgG per unit of surface area. **C** Kinetics of antibody adsorption in the different capillary surfaces using 40  $\mu\text{g}/\text{ml}$  of mouse IgG in solution; to enable direct comparison of capillaries having different inner diameters, surface coverage has been normalised with SAV ratio. The continuous lines in the B represent the values estimated with Langmuir model (equation 2), with best-fitted parameters summarised in Table 3, whereas in C represents the best-fitted kinetic model (equation 3), with best-fitted parameters summarised in Table 4.

Equilibrium adsorption of IgG onto Teflon® FEP and LLDPE was very similar, as seen from the almost overlapping Langmuir isotherms in Figure 5B and best-fitted Langmuir parameters (Table 3). This is due presumably to similar hydrophobicity of the two polymers, showing a contact angle with water of 123°<sup>22</sup> and 120°<sup>23</sup> respectively.<sup>21</sup> However, it contrasted with the Langmuir isotherms obtained for the glass capillaries having a contact angle ~25°<sup>24</sup> which showed 2 to 4-fold larger mass of antibody adsorbed per surface area available based on data shown in both Figure 5B and Figure 5C. Although we have not extensively tested other capillary surfaces in this study, these original results suggest antibody adsorption is very distinct between hydrophobic and hydrophilic surfaces. Some studies reported a higher mass of protein adsorbed onto hydrophilic surfaces, such as bare glass, compared to hydrophobic surfaces such as plastic,<sup>43,44</sup> this is further supported by our data. Note however that the larger surface density obtained with the glass capillaries means antibody adsorption on glass surfaces occurs in multilayers, which is undesirable in affinity biorecognition and in particular heterogeneous immunoassays. Consequently, covalent immobilisation is a preferred strategy for preparation of glass immuno-surfaces.

**Table 2.** IgG adsorption kinetic parameters (based on equation 3 and data plotted in Figure 4A) for Teflon® FEP microcapillaries

IgG bulk (M)	$K_{on}$ (M <sup>-1</sup> min <sup>-1</sup> )	$K_{off}$ (min <sup>-1</sup> )	R <sup>2</sup>
<b>1.3x10<sup>-7</sup> (20 µg/ml)</b>	5.01×10 <sup>5</sup>	2.76×10 <sup>-1</sup>	0.9556
<b>2.6x10<sup>-7</sup> (40 µg/ml)</b>	2.69×10 <sup>5</sup>	1.30×10 <sup>-1</sup>	0.9811
<b>1.3x10<sup>-6</sup> (200 µg/ml)</b>	1.1×10 <sup>6</sup>	1.78×10 <sup>-1</sup>	0.9345

**Table 3.** Best-fitted parameters for Langmuir isotherms (based on equation 2 and plotted in Figure 5B) describing antibody adsorption in different microcapillary materials. Note in this case  $\tau_{max}$  in equation 2 was computed as ratio of percentage of surface coverage,  $\Phi$  to SAV

	Teflon® FEP	LDPE	Glass
<b><math>K</math> (ml/µg)</b>	0.014	0.016	0.004
<b><math>\tau_{max}</math> (shown as percentage <math>\Phi</math>/SAV, cm)</b>	0.55	0.57	2.15
<b>R<sup>2</sup></b>	0.9963	0.9982	0.9939

The reduced affinity of antibodies for hydrophobic surfaces favours the formation of less dense layers that are actually preferred for sensitive ELISA, as surface coverage affects antibody activity/orientation and smaller amounts of adsorbed antibody encourages a stronger attachment of molecules to the surface.<sup>35,45</sup> In contrast, antibody adsorption onto hydrophilic surfaces yields higher mass adsorbed with the possible formation of antibody multilayers, due to electrostatic interactions between antibodies and hydrophilic surfaces.<sup>46</sup> Also, higher mass of adsorbed antibody promotes easy desorption from the glass surfaces as a result of reduced conformational changes.<sup>39,40</sup> For these reasons hydrophobic surfaces are usually preferred for antibody adsorption in diagnostic test surfaces as immobilised antibodies are more resistant to surfactants and present lower desorption due to irreversible binding between antibody and surface, which is essential for heterogeneous assays.<sup>36,41,47</sup> Note we have extensively washed the capillaries with 0.05% PBS-Tween in all experimental sets shown herein. The irreversibility was related to the conformational changes that part of the antibody undergoes when adsorbed to a hydrophobic surface. Multiple experimental replicas confirmed (data not shown) showed no detectable loss of antibody with the washings. Our data suggested Teflon® FEP microcapillaries present a highly hydrophobic surface, which favours the irreversible nature of antibodies on the surface.<sup>43,45</sup>

In line with previous studies, surface chemistry affected antibody adsorption kinetics, being the adsorption equilibrium reached in less than 5 minutes for glass surfaces, within 10 minutes for Teflon®FEP and take up to 30 minutes for LLDPE (Figure 5C and Table 4).

**Table 4.** IgG adsorption kinetic parameters (equation 3 and data plotted in Figure 5B) for different capillary surfaces, based on IgG bulk concentration of 40 µg/ml

	$K_{on}$ ( $M^{-1} \text{ min}^{-1}$ )	$K_{off}$ ( $\text{min}^{-1}$ )	$R^2$
<b>Teflon® FEP</b>	$2.69 \times 10^5$	$1.30 \times 10^{-1}$	0.9761
<b>LDPE</b>	$1.14 \times 10^5$	$1.00 \times 10^{-1}$	0.9610
<b>Glass</b>	$2.94 \times 10^6$	1.96	0.9634

Antibody adsorbed faster to glass surfaces with an association constant  $K_{on}$  around one order of magnitude larger than for the plastic surfaces studied (Table 4), which can be explained by electrostatic interactions between the antibodies and glass surfaces. Note that values for the dissociation constant,  $K_{off}$  for antibody adsorption were also one order of magnitude larger in



1  
2  
3 glass capillaries, which agrees with the reversibility of antibodies adsorbed to hydrophilic  
4 surfaces. This is another reason why glass immuno-surfaces tend to imply surface  
5 modification strategies and antibody covalent binding for formation of a bio-recognition  
6 monolayer.  
7  
8  
9

## 10 11 12 13 **5. CONCLUSIONS**

14  
15 In spite of the uniqueness of FEP Teflon® (excellent optical transparency, electrostatic and  
16 very high contact angle for water) and its “non-sticky” properties, FEP Teflon®  
17 microcapillaries revealed to form an optimal bio-recognition monolayer, with antibodies  
18 biologically active and irreversible bound to the surface, enabling robust and sensitive  
19 optical, quantitative diagnostic testing to be carried out. Passive adsorption of antibodies into  
20 FEP microfluidic strips showed insensitive to the temperature of incubation and ionic buffer  
21 strength, with a neutral pH favouring robustness in performance. In addition, antibody  
22 kinetics onto FEP microcapillaries revealed fast, taking up to 10 minutes to reach  
23 equilibrium, with no differences in assays performance. These features are important for the  
24 lowering the cost of the diagnostic strips manufacturing process, since it removes the need of  
25 precise temperature control, enables a higher degree of freedom to operators and allows high  
26 throughput production. Highly sensitive, optical, sandwich assays are possible in FEP  
27 Teflon® strips due to the irreversibility of antibodies adsorption to the surface and by the  
28 modest antibody surface packing densities, observed as between 45 to 69% for optimal  
29 antibody activity.  
30  
31  
32  
33  
34  
35  
36  
37  
38  
39  
40  
41

## 42 **ASSOCIATED CONTENT**

### 43 44 **Supporting Information**

45  
46 The Supporting Information is available free of charge on the ACS Publications website at  
47 DOI: xxx.  
48

49  
50       Supplementary methodology and results, including additional Tables S1 and S2  
51

## 52 **AUTHOR INFORMATION**

### 53 54 **Corresponding Author**

55  
56 \*Email [n.m.reis@bath.ac.uk](mailto:n.m.reis@bath.ac.uk). Tel. +44 (0)1225 383 369 (N.M. Reis).  
57

### 58 59 **ORCID**

60

1  
2  
3 Nuno M. Reis: 0000-0002-8706-6998  
4  
5

## 6 **ACKNOWLEDGEMENTs**

7 The authors are grateful to Patrick Hester for donating the MCF material and to  
8 Loughborough University for funding this study.  
9  
10

## 11 **ABBREVIATIONS**

12 FEP, Fluorinated ethylene propylene; LLDPE, linear low-density polyethylene, IgG,  
13 immunoglobulin G; capAb, capture antibody; POC, point of care; PDMS,  
14 Polydimethylsiloxane; PTFE, Polytetrafluoroethylene; MCF, microcapillary film; PSA,  
15 prostate specific antigen; IL-1 $\beta$ , interleukin-1 beta; ELISA, Enzyme-Linked Immunosorbent  
16 Assay; BSA, bovine serum albumin; PBS, phosphate buffer saline; HEPES, 4(2-  
17 hydroxyethyl)-1-piperazineethanesulfonic acid; BCA, bicinchoninic acid assay; HRP,  
18 horseradish peroxidase; OPD, o-phenylenediamine; Abs, absorbance.  
19  
20  
21  
22  
23  
24  
25

## 26 **REFERENCES**

- 27  
28  
29 (1) Rabe, M.; Verdes, D.; Seeger, S. Understanding Protein Adsorption Phenomena at  
30 Solid Surfaces. *Adv. Colloid Interface Sci.* **2011**, *162* (1–2), 87–106.  
31 <https://doi.org/10.1016/j.cis.2010.12.007>.  
32  
33 (2) Kim, D.; Herr, A. E. Protein Immobilization Techniques for Microfluidic Assays.  
34 *Biomicrofluidics* **2013**, *7* (4), 41501. <https://doi.org/10.1063/1.4816934>.  
35  
36 (3) Trilling, A. K.; Beekwilder, J.; Zuilhof, H. Antibody Orientation on Biosensor  
37 Surfaces: A Minireview. *Analyst* **2013**, *138* (6), 1619.  
38 <https://doi.org/10.1039/c2an36787d>.  
39  
40 (4) Buijs, J.; Norde, W.; Lichtenbelt, J. W. T. Changes in the Secondary Structure of  
41 Adsorbed IgG and F(Ab')<sub>2</sub> Studied by FTIR Spectroscopy. *Langmuir* **1996**, *12* (6),  
42 1605–1613. <https://doi.org/10.1021/la950665s>.  
43  
44 (5) Tajima, N.; Takai, M.; Ishihara, K. Significance of Antibody Orientation Unraveled:  
45 Well-Oriented Antibodies Recorded High Binding Affinity. *Anal. Chem.* **2011**, *83* (6),  
46 1969–1976. <https://doi.org/10.1021/ac1026786>.  
47  
48 (6) Jung, Y.; Jeong, J. Y.; Chung, B. H. Recent Advances in Immobilization Methods of  
49 Antibodies on Solid Supports. <https://doi.org/10.1039/b800014j>.  
50  
51 (7) Davies, C. Introduction to Immunoassay Principles. In *The Immunoassay Handbook*;  
52 Wild, D., Ed.; Elsevier Ltd.: Oxford, 2005; pp 34–38.  
53  
54 (8) Deshpande, S. S. *Enzyme Immunoassays: From Concept to Product Development*;  
55 Springer Science & Business Media, 1996.  
56  
57 (9) Lin, C.-C.; Wang, J.-H.; Wu, H.-W.; Lee, G.-B. Microfluidic Immunoassays. *J. Assoc.*  
58 *Lab. Autom.* **2010**, *15* (3), 253–274. <https://doi.org/10.1016/j.jala.2010.01.013>.  
59  
60 (10) Ng, A. H. C.; Uddayasankar, U.; Wheeler, A. R. Immunoassays in Microfluidic  
Systems. *Anal. Bioanal. Chem.* **2010**, *397* (3), 991–1007.

- 1  
2  
3 <https://doi.org/10.1007/s00216-010-3678-8>.
- 4  
5 (11) Nakanishi, K.; Sakiyama, T.; Imamura, K. On the Adsorption of Proteins on Solid  
6 Surfaces, a Common but Very Complicated Phenomenon. *J. Biosci. Bioeng.* **2001**, *91*  
7 (3), 233–244. [https://doi.org/10.1016/S1389-1723\(01\)80127-4](https://doi.org/10.1016/S1389-1723(01)80127-4).
- 8  
9 (12) Barbosa, A. I. The Development and Optimisation of a Novel Microfluidic  
10 Immunoassay Platform for Point of Care Diagnostics, Loughborough University, 2015.
- 11  
12 (13) Salim, M.; O’Sullivan, B.; McArthur, S. L.; Wright, P. C. Characterization of  
13 Fibrinogen Adsorption onto Glass Microcapillary Surfaces by ELISA. *Lab Chip* **2007**,  
14 *7* (1), 64–70. <https://doi.org/10.1039/b612521m>.
- 15  
16 (14) Barbosa, A. I.; Gehlot, P.; Sidapra, K.; Edwards, A. D.; Reis, N. M. Portable  
17 Smartphone Quantitation of Prostate Specific Antigen (PSA) in a Fluoropolymer  
18 Microfluidic Device. *Biosens. Bioelectron.* **2015**, *70*, 5–14.  
19 <https://doi.org/10.1016/j.bios.2015.03.006>.
- 20  
21 (15) Castanheira, A. P.; Barbosa, A. I.; Edwards, A. D.; Reis, N. M. Multiplexed  
22 Femtomolar Quantitation of Human Cytokines in a Fluoropolymer Microcapillary  
23 Film. *Analyst* **2015**, *140* (16), 5609–5618. <https://doi.org/10.1039/c5an00238a>.
- 24  
25 (16) Barbosa, A. I.; Castanheira, A. P.; Edwards, A. D.; Reis, N. M. A Lab-in-a-Briefcase  
26 for Rapid Prostate Specific Antigen (PSA) Screening from Whole Blood. *Lab Chip*  
27 **2014**. <https://doi.org/10.1039/c4lc00464g>.
- 28  
29 (17) Alves, I. P.; Reis, N. M. Immunocapture of Escherichia Coli in a Fluoropolymer  
30 Microcapillary Array. *J. Chromatogr. A* **2018**.  
31 <https://doi.org/10.1016/J.CHROMA.2018.11.067>.
- 32  
33 (18) Hallmark, B.; Gadala-Maria, F.; Mackley, M. R. The Melt Processing of Polymer  
34 Microcapillary Film (MCF). *J. Nonnewton. Fluid Mech.* **2005**, *128* (2–3), 83–98.  
35 <https://doi.org/10.1016/j.jnnfm.2005.03.013>.
- 36  
37 (19) Barbosa, A. I.; Castanheira, A. P.; Reis, N. M. Sensitive Optical Detection of  
38 Clinically Relevant Biomarkers in Affordable Microfluidic Devices: Overcoming  
39 Substrate Diffusion Limitations. *Sensors Actuators B Chem.* **2018**, *258*, 313–320.  
40 <https://doi.org/10.1016/J.SNB.2017.11.086>.
- 41  
42 (20) Pivetal, J.; Pereira, F. M.; Barbosa, A. I.; Castanheira, A. P.; Reis, N. M.; Edwards, A.  
43 D. Covalent Immobilisation of Antibodies in Teflon-FEP Microfluidic Devices for the  
44 Sensitive Quantification of Clinically Relevant Protein Biomarkers. *Analyst* **2017**, *142*  
45 (6), 959–968. <https://doi.org/10.1039/c6an02622b>.
- 46  
47 (21) Edwards, A. D.; Reis, N. M.; Slater, N. K. H.; Mackley, M. R. A Simple Device for  
48 Multiplex ELISA Made from Melt-Extruded Plastic Microcapillary Film. *Lab Chip*  
49 **2011**, *11* (24), 4267–4273. <https://doi.org/10.1039/c0lc00357c>.
- 50  
51 (22) Reis, N. M.; Pivetal, J.; Loo-Zazueta, A. L.; Barros, J. M. S.; Edwards, A. D. Lab on a  
52 Stick: Multi-Analyte Cellular Assays in a Microfluidic Dipstick. *Lab Chip* **2016**, *16*  
53 (15), 2891–2899. <https://doi.org/10.1039/C6LC00332J>.
- 54  
55 (23) Fu, Z.; Liu, M.; Xu, J.; Wang, Q.; Fan, Z. Surface Modification of Linear Low-Density  
56 Polyethylene Film by Amphiphilic Graft Copolymers Based on Poly(Higher  $\alpha$ -Olefin)-  
57 Graft-Poly(Ethylene Glycol). *J. Appl. Polym. Sci.* **2011**, *119* (2), 1111–1121.  
58 <https://doi.org/10.1002/app.32819>.
- 59  
60 (24) Sumner, A. L.; Menke, E. J.; Dubowski, Y.; Newberg, J. T.; Penner, R. M.;  
Hemming, J. C.; Wingen, L. M.; Brauers, T.; Finlayson-Pitts, B. J. The Nature of

- 1  
2  
3 Water on Surfaces of Laboratory Systems and Implications for Heterogeneous  
4 Chemistry in the Troposphere. <https://doi.org/10.1039/b308125g>.
- 5  
6 (25) Silverton, E. W.; Navia, M. A.; Davies, D. R. Three-Dimensional Structure of an Intact  
7 Human Immunoglobulin. *Proc. Natl. Acad. Sci. U. S. A.* **1977**, *74* (11), 5140–5144.
- 8  
9 (26) Norde, W. Protein Adsorption at Solid Surfaces: A Thermodynamic Approach. 1994.
- 10  
11 (27) Hlady, V.; Buijs, J. Protein Adsorption on Solid Surfaces. *Curr. Opin. Biotechnol.*  
12 **1996**, *7* (1), 72–77.
- 13  
14 (28) Lee, S.; Park, J.-S.; Lee, T. R. The Wettability of Fluoropolymer Surfaces: Influence  
15 of Surface Dipoles. **2008**. <https://doi.org/10.1021/la700902h>.
- 16  
17 (29) Chen, W. Y.; Huang, H. M.; Lin, C. C.; Lin, F. Y.; Chan, Y. C. Effect of Temperature  
18 on Hydrophobic Interaction between Proteins and Hydrophobic Adsorbents: Studies  
19 by Isothermal Titration Calorimetry and the van't Hoff Equation. *Langmuir* **2003**, *19*  
20 (22), 9395–9403. <https://doi.org/10.1021/la034783o>.
- 21  
22 (30) Abraham, G. N.; Podell, D. N.; Wistar, R.; Johnston, S. L.; Welch, E. H.; Welch, E. H.  
23 Immunological and Structural Properties of Human Monoclonal IgG Cryoglobulins.  
24 *Clin. Exp. Immunol.* **1979**, *36* (1), 63–70.
- 25  
26 (31) van Oss, C. J. A Review of “ Inter-molecular and Surface Forces, Second Edition.  
27 Jacob N. Israelachvili. Academic Press, London, 1991. Pp. Xxi + 450; Hardbound,  
28 \$49.95. *J. Dispers. Sci. Technol.* **1992**, *13* (6), 718–719.  
29 <https://doi.org/10.1080/01932699208943350>.
- 30  
31 (32) Wright, G. G.; Schomaker, V. Studies on the Denaturation of Antibody. IV. The  
32 Influence of PH and Certain Other Factors on the Rate of Inactivation of  
33 Staphylococcus Antitoxin in Urea Solutions. *Journal of Biological Chemistry.*  
34 American Society for Biochemistry and Molecular Biology August 1948, pp 169–177.
- 35  
36 (33) Jones, K. L.; O'Melia, C. R. Protein and Humic Acid Adsorption onto Hydrophilic  
37 Membrane Surfaces: Effects of PH and Ionic Strength. *J. Memb. Sci.* **2000**, *165* (1),  
38 31–46. [https://doi.org/10.1016/S0376-7388\(99\)00218-5](https://doi.org/10.1016/S0376-7388(99)00218-5).
- 39  
40 (34) Zhao, X.; Pan, F.; Garcia-Gancedo, L.; Flewitt, A. J.; Ashley, G. M.; Luo, J.; Lu, J. R.  
41 Interfacial Recognition of Human Prostate-Specific Antigen by Immobilized  
42 Monoclonal Antibody: Effects of Solution Conditions and Surface Chemistry. *J. R.*  
43 *Soc. Interface* **2012**, *9* (75), 2457–2467. <https://doi.org/10.1098/rsif.2012.0148>.
- 44  
45 (35) Vörös, J. The Density and Refractive Index of Adsorbing Protein Layers. *Biophys. J.*  
46 **2004**, *87* (1), 553–561. <https://doi.org/10.1529/biophysj.103.030072>.
- 47  
48 (36) Wiseman, M. E.; Frank, C. W. Antibody Adsorption and Orientation on Hydrophobic  
49 Surfaces. *Langmuir* **2012**, *28* (3), 1765–1774. <https://doi.org/10.1021/la203095p>.
- 50  
51 (37) Xu, H.; Lu, J. R.; Williams, D. E. Effect of Surface Packing Density of Interfacially  
52 Adsorbed Monoclonal Antibody on the Binding of Hormonal Antigen Human  
53 Chorionic Gonadotrophin. *J. Phys. Chem. B* **2006**, *110* (4), 1907–1914.  
54 <https://doi.org/10.1021/jp0538161>.
- 55  
56 (38) Buijs, J.; Lichtenbelt, J. W. T.; Norde, W.; Lyklema, J. Adsorption of Monoclonal  
57 IgGs and Their F(Ab')<sub>2</sub> Fragments onto Polymeric Surfaces. *Colloids Surfaces B*  
58 *Biointerfaces* **1995**, *5* (1–2), 11–23. [https://doi.org/10.1016/0927-7765\(95\)98205-2](https://doi.org/10.1016/0927-7765(95)98205-2).
- 59  
60 (39) Vermeer, A. W. P.; Bremer, M. G. E. G.; Norde, W. Structural Changes of IgG  
Induced by Heat Treatment and by Adsorption onto a Hydrophobic Teflon Surface  
Studied by Circular Dichroism Spectroscopy. *Biochim. Biophys. Acta - Gen. Subj.*

- 1  
2  
3       **1998**, *1425* (1), 1–12.  
4  
5 (40) Vermeer, A. Adsorption of IgG onto Hydrophobic Teflon. Differences between the  
6 Fab and Fc Domains. *Biochim. Biophys. Acta - Gen. Subj.* **2001**, *1526* (1), 61–69.  
7 [https://doi.org/10.1016/S0304-4165\(01\)00101-5](https://doi.org/10.1016/S0304-4165(01)00101-5).  
8  
9 (41) Xu, H.; Lu, J. R.; Williams, D. E. Effect of Surface Packing Density of Interfacially  
10 Adsorbed Monoclonal Antibody on the Binding of Hormonal Antigen Human  
11 Chorionic Gonadotrophin. *J. Phys. Chem. B* **2006**, *110* (4), 1907–1914.  
12 <https://doi.org/10.1021/jp0538161>.  
13  
14 (42) Wiseman, M. E.; Frank, C. W. Antibody Adsorption and Orientation on Hydrophobic  
15 Surfaces. *Langmuir* **2012**, *28* (3), 1765–1774. <https://doi.org/10.1021/la203095p>.  
16  
17 (43) Jönsson, U.; Ivarsson, B.; Lundström, I.; Berghem, L. Adsorption Behavior of  
18 Fibronectin on Well-Characterized Silica Surfaces. *J. Colloid Interface Sci.* **1982**, *90*  
19 (1), 148–163. [https://doi.org/10.1016/0021-9797\(82\)90408-8](https://doi.org/10.1016/0021-9797(82)90408-8).  
20  
21 (44) Zangmeister, R. A. Application of X-Ray Photoelectron Spectroscopic Analysis to  
22 Protein Adsorption on Materials Relevant to Biomanufacturing. *J. Pharm. Sci.* **2012**,  
23 *101* (4), 1639–1644. <https://doi.org/10.1002/jps.23023>.  
24  
25 (45) Sethuraman, A.; Han, M.; Kane, R. S.; Belfort, G. Effect of Surface Wettability on the  
26 Adhesion of Proteins. *Langmuir* **2004**, *20* (18), 7779–7788.  
27 <https://doi.org/10.1021/la049454q>.  
28  
29 (46) Couston, R. G.; Skoda, M. W.; Uddin, S.; van der Walle, C. F. Adsorption Behavior of  
30 a Human (1) Couston, R. G.; Skoda, M. W.; Uddin, S.; van Der Walle, C. F.  
31 Adsorption Behavior of a Human Monoclonal Antibody at Hydrophilic and  
32 Hydrophobic Surfaces. *MAbs* **5**, 126–139. Monoclonal Antibody at Hydrophilic and  
33 Hydrophobic. *MAbs* **5** (1), 126–139. <https://doi.org/10.4161/mabs.22522>.  
34  
35 (47) Oom, A.; Poggi, M.; Wikström, J.; Sukumar, M. Surface Interactions of Monoclonal  
36 Antibodies Characterized by Quartz Crystal Microbalance with Dissipation: Impact of  
37 Hydrophobicity and Protein Self-Interactions. *J. Pharm. Sci.* **2012**, *101* (2), 519–529.  
38 <https://doi.org/10.1002/jps.22771>.  
39  
40  
41  
42  
43  
44  
45  
46  
47  
48  
49  
50  
51  
52  
53  
54  
55  
56  
57  
58  
59  
60

## TOC graphic

